# Supporting Information

## CuCoNi-S anchored $CoMoO_4/MoO_3$ forming core-shell structure for high-performance asymmetric supercapacitor

Tiansheng Li,[a] Zhifeng Zhao,*[b] Zhanhua Su,[b] Rui Sun,[a] Xiaofeng Li,*[a] and Yongchen Shang,*[a]

[a]*College of Chemistry and Chemical Engineering, Harbin Normal University, Harbin, 150025, China*

[b] *College of Chemistry, Guangdong University of Petrochemical Technology, Maoming, 525000, China*

*Corresponding author E-mail: zhifengzhao1980@163.com; lixiaofeng@hrbnu.edu.cn; yongchenshang@163.com*

## I. Experimental Section

### 1. Materials and Characterizations

All reagents are commercially available and used as received without further purification. Pattern X-ray diffraction (XRD) was recorded using a Bruke D8 equipped with Cu-Ka radiation. X-ray photon-electron Spectroscopy (XPS) analysis was performed using a VG ESCALAB MK II spectrophotometer with Mg-Kα radiation (1253.6 eV). Scanning electron microscopy (SEM) test was carried out on a Hitachi S-4800 instrument at an accelerating voltage of 5 kV. The compositions of the products were examined using energy dispersive X-ray spectroscopy (EDX) attached to the EM system. The transmission electron microscopy (TEM), high resolution transmission electron microscopy (HRTEM) and selected area electron diffraction (SAED) patterns was performed on a FEI Talos-F200S electron microscope. Specific surface areas and pore size were measured using Brunauer-Emmett-Teller (BET).

### 2. Pretreatment of nickel foam

Immerse the nickel foam in a 1:3 HCl solution for 20 min to remove the oxide film on the surface, then sonicate with deionized water (DI) for 30 min 3 times to remove the residual hydrochloric acid on the surface, and finally sonicate with ethanol for 20 min to remove the organic matter on the surface of the nickel foam.

### 3. Synthesis of $CoMoO_4/MoO_3$

The $CoMoO_4/MoO_3$ was prepared by hydrothermal process. The $Co(NO_3)_2•6H_2O$ (0.7276 g, 2.500 mmol) and $Na_2MoO_4$ (0.3024 g, 1.469 mmol) were added to deionized water (15 mL) and stirred for 30 min to make it dispersed evenly. The solution was dumped into a stainless steel reactor (25 mL), and then a slice of pretreated NF (geometric surface area, 1 × 2 $cm^2$ ) was added to the reactor at the same time at 140 °C for 5 h, then cooling to room temperature, NF containing the purple products was rinsed with the same water and dried in 60 °C.

### 4. Synthesis of $CoMoO_4/MoO_3$@CuCoNi-S

The $CoMoO_4/MoO_3$@CuCoNi-S was synthesized by electrodeposition approach. In a typical synthesis, $Co(NO_3)_2•6H_2O$(1.1641 g, 3.999 mmol), $Ni(NO_3)_2•6H_2O$ (0.2908 g, 1.000 mmol), $Cu(NO_3)_2•3H_2O$ (0.2416 g, 1.000 mmol) and thiourea (TU) (0.6090 g,

8.000 mmol) were dissolved in deionized water (50 mL) and stirred for 30 min. Which was served as an electrolyte solution. NF with $CoMoO_4/MoO_3$ was chosen as the working electrode, Ag/AgCl electrode and Pt plate were served as the reference electrode and counter electrode, respectively. For uniform deposition of the CuCoNi-S layer on the substrate, the electrode is synthesized using 8 cycles with potentials ranging from − 1.2 to + 0.2 V, the scan speed is 5 mV $s^{-1}$. Repeating rinse with deionized water and dry overnight in vacuum at 60 °C for the sample. The $CoMoO_4/MoO_3$@CuCoNi-S loaded on the NF is about 1.2 mg $cm^{-2}$.

**5. Synthesis of CuCoNi-S**

The electrodeposition process of CuCoNi-S and $CoMoO_4/MoO_3$@CuCoNi-S is basically the same, except that the working electrode is pretreated NF.

**6. Electrochemical measurements**

Electrochemical performance tests were performed using the CHI760E electrochemical workstation under a three-electrode system. The resulting nickel foam was used directly as the working electrode, platinum foil and Ag/AgCl as counter electrodes and reference electrodes, respectively, and 3M KOH aqueous solution as electrolyte. Cyclic voltammetry (CV) curves were performed in the potential range of 0 to 0.6 V, with scan rates of 5, 10, 20, 30, 50, and 80 mV $s^{-1}$, respectively. The galvanostatic charge/discharge (GCD) measurements were performed in potential windows of 0-0.4 V, with current densities of 1, 2, 3, 5, 8, and 10 A $g^{-1}$, respectively.

The specific capacitance of the active material is calculated according to the following formula:

$$C_{sp} = I * \Delta t / m * \Delta V$$

where $C_{sp}$, I, Δt, m and ΔV represent the specific capacitance (F $g^{-1}$), the discharge current (A), the discharge time (s), the mass of the active material (g) and the potential windows (V), respectively.

In the preparation process of asymmetric supercapacitors, $CoMoO_4/MoO_3$@CuCoNi-S and activated carbon (AC) electricity are used as positive

and negative electrodes, respectively. The separator is cellulose paper and the electrolyte is PVA/KOH. Voltammetry charges (Q) can be evaluated as follows:

$$Q=C_{sp}\times\Delta V\times m$$

Where C represents the specific capacitance of a single electrode (F $g^{-1}$), ΔV is the potential window (V) for each electrode, and m is the load mass for each electrode (g). To balance the positive and negative charges of the supercapacitor, the voltammetry charges of the positive and negative electrodes follow the equation: $Q_+=Q_-$. Therefore, the mass ratio of the positive and negative electrodes is calculated as follows:

$$m_+/m_-=(C_-\times\Delta V_-)/(C_+\times\Delta V_+)$$

The power density and energy density of supercapacitors can be calculated according to the following formula：

$$E=C_{sp}\times\Delta V^2/7.2$$

$$P = 3600E / \Delta t$$

Where $C_{sp}$ represents the specific capacitance (F $g^{-1}$) and ΔV represents the potential windows (V); Δt is the discharge time(s).

## II Supplementary Structural Section

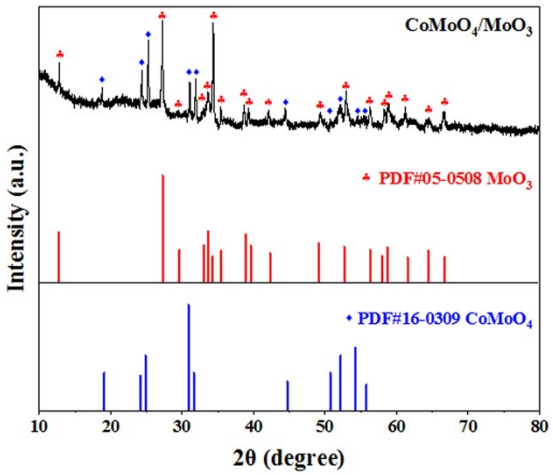


**Fig.S1** XRD patterns of $CoMoO_4/MoO_3$, $MoO_3$ and $CoMoO_4$.

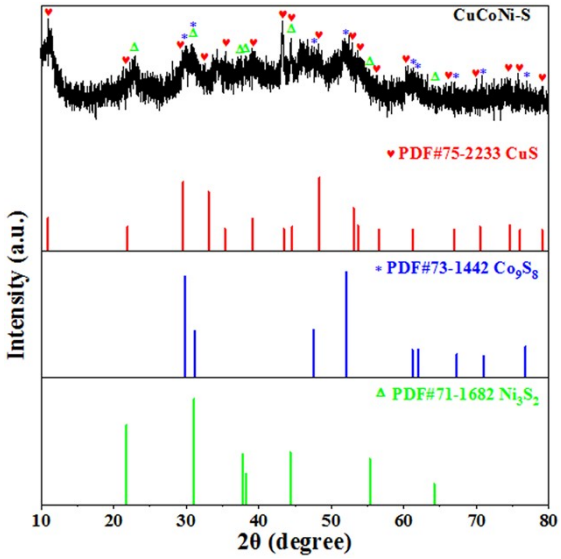


**Fig.S2** XRD patterns of CuCoNi-S, CuS, $Co_9S_8$ and $Ni_3S_2$.

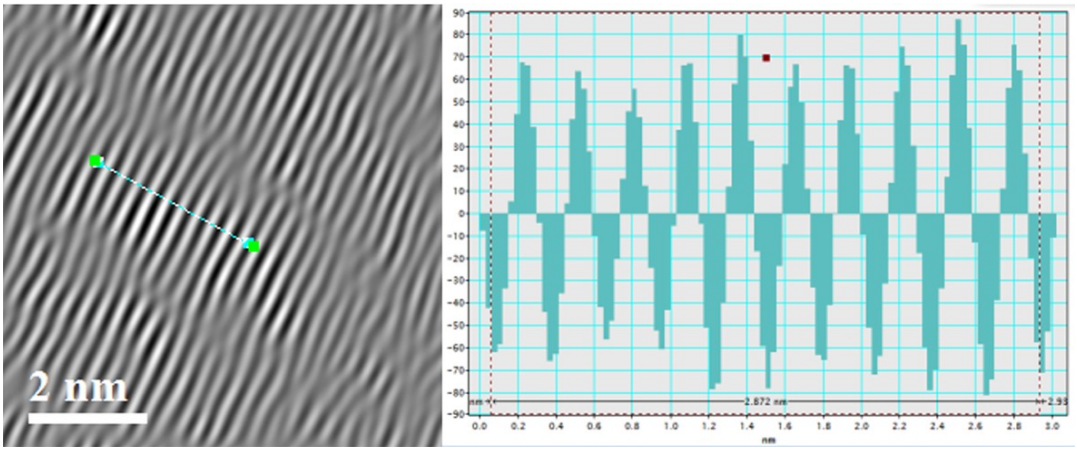


**Fig.S3** The plot profiles for the interplanar spacings of $Co_9S_8$.

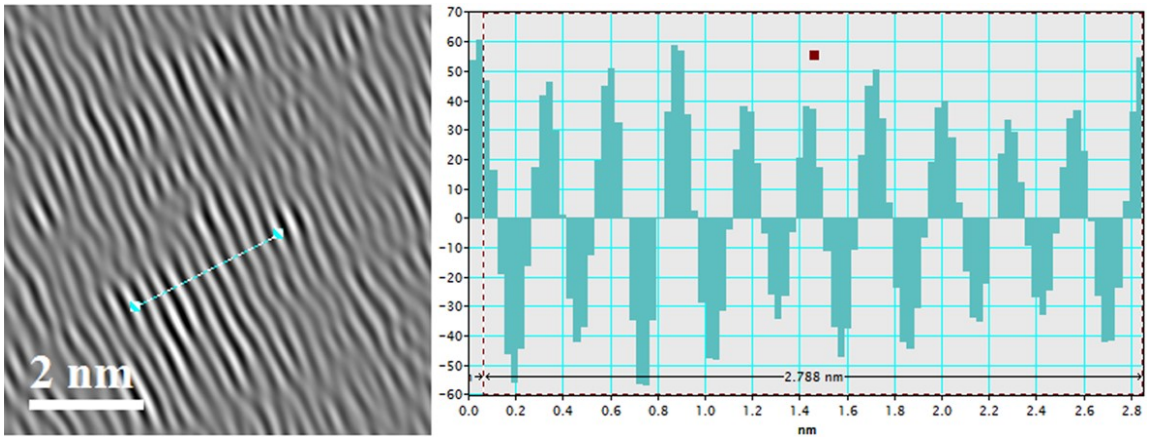


**Fig.S4** The plot profiles for the interplanar spacings of CuS.

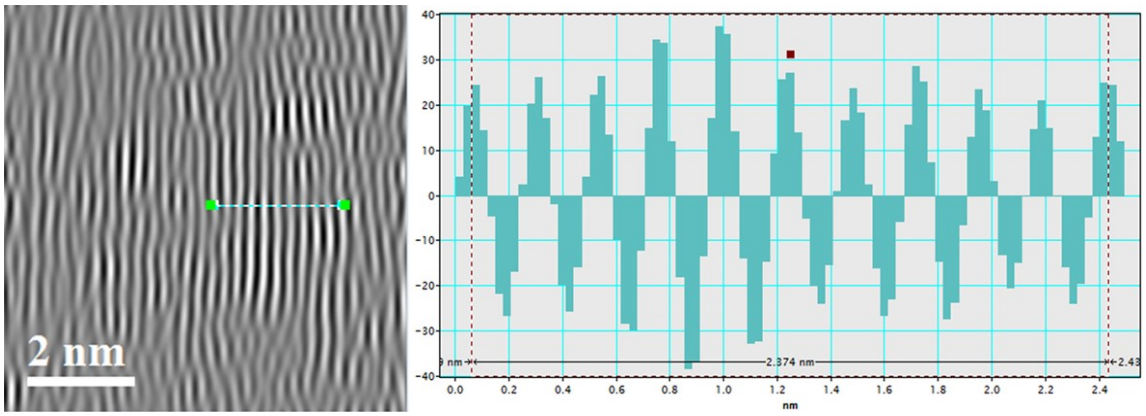


**Fig.S5** The plot profiles for the interplanar spacings of $Ni_3S_2$.

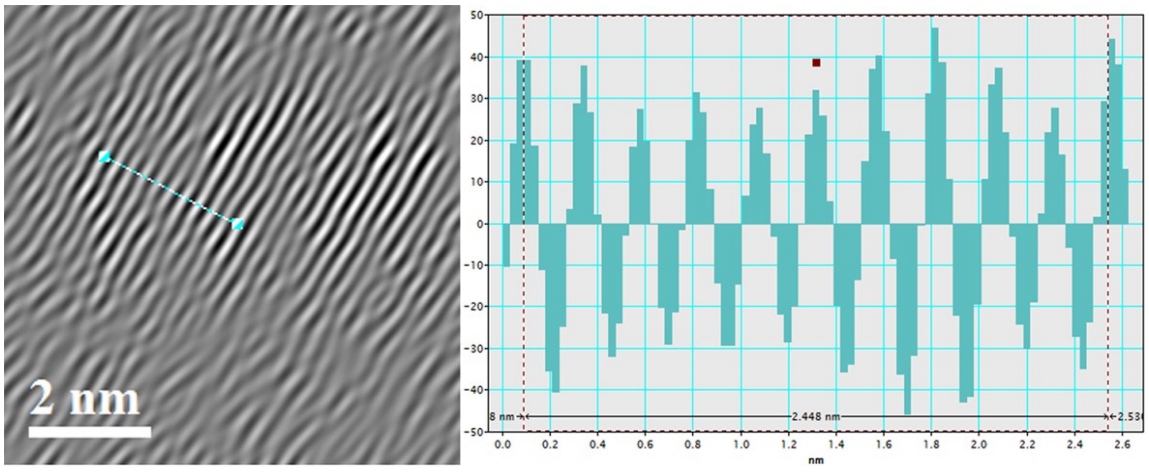


**Fig.S6** The plot profiles for the interplanar spacings of $CoMoO_4$.

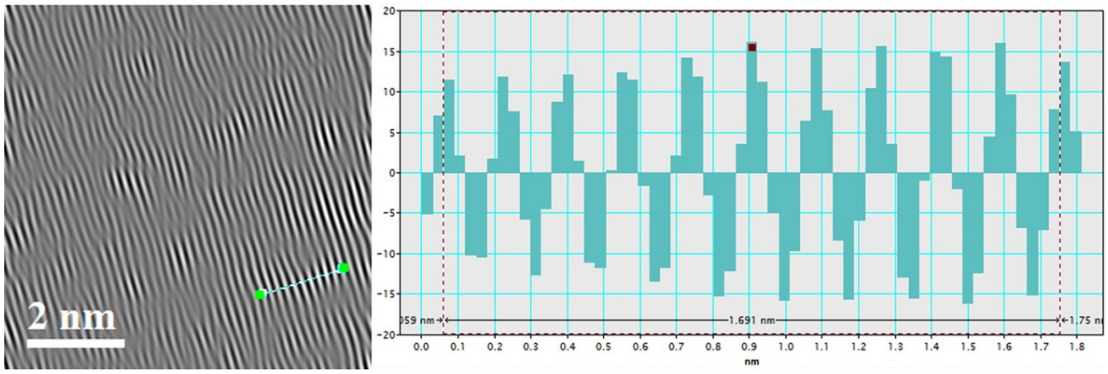


**Fig.S7** The plot profiles for the interplanar spacings of $MoO_3$.

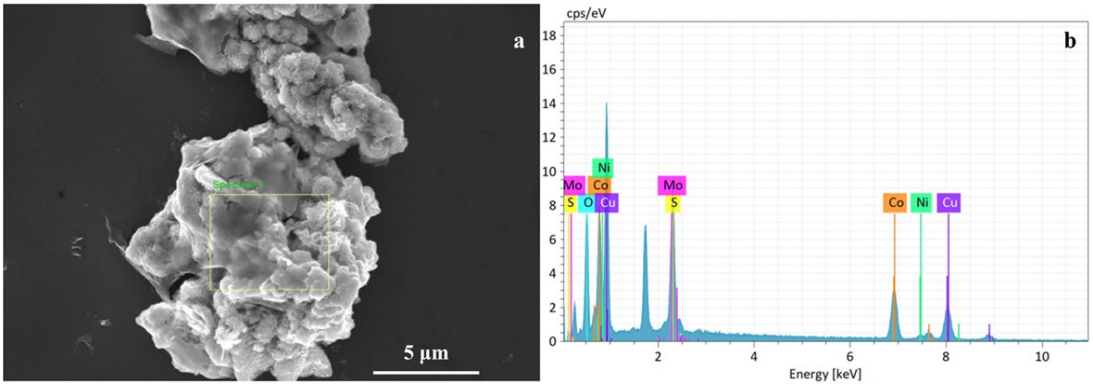


**Fig. S8** (a) SEM image (b) EDAX spectrum of $CoMoO_4/MoO_3$@CuCoNi-S.

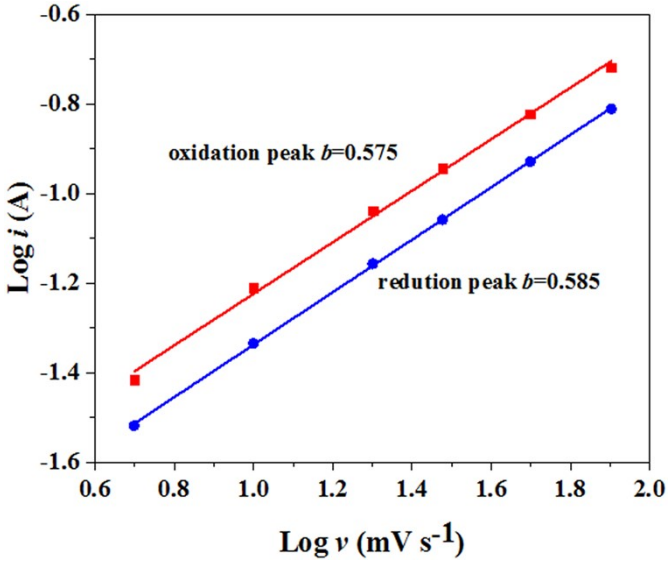


**Fig.S9** Straight line relationship of log*i* and log*v* of $CoMoO_4/MoO_3$ electrode.

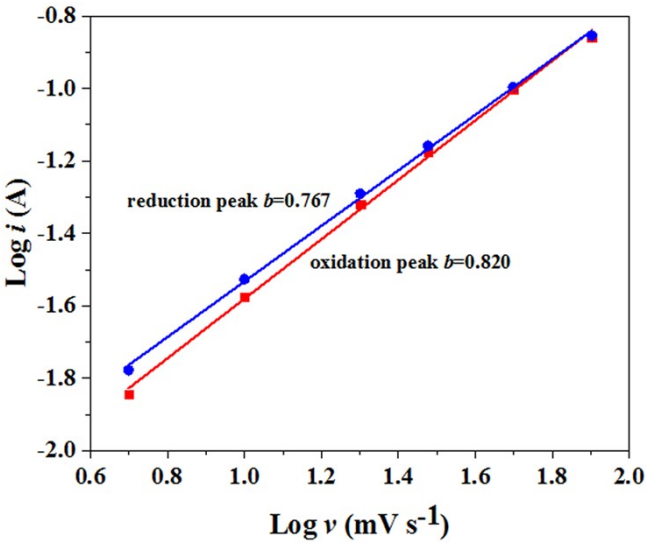


**Fig.S10** Straight line relationship of log*i* and log*v* of CuCoNi-S electrode.

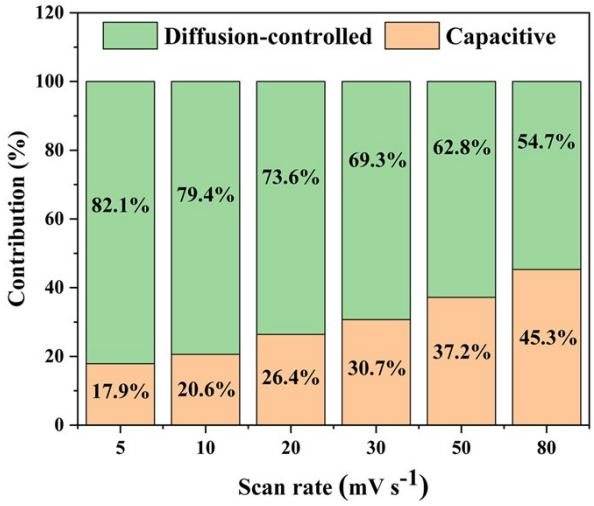


**Fig.S11** Normalized contribution ratio of capacitive capcacities at different scan rates of $CoMoO_4/MoO_3$ electrode.

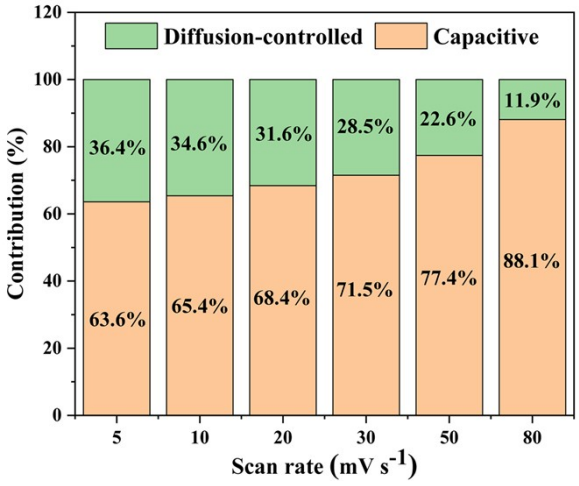


**Fig.S12** Normalized contribution ratio of capacitive capcacities at different scan rates of CuCoNi-S electrode.

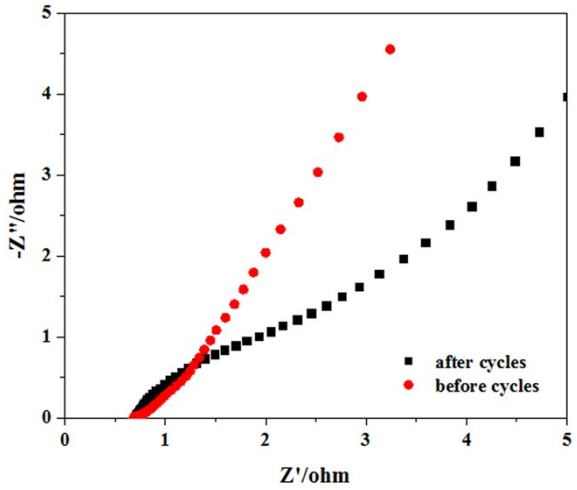


**Fig. S13** Nyquist plots of before and after cycles for $CoMoO_4/MoO_3$@CuCoNi-S.

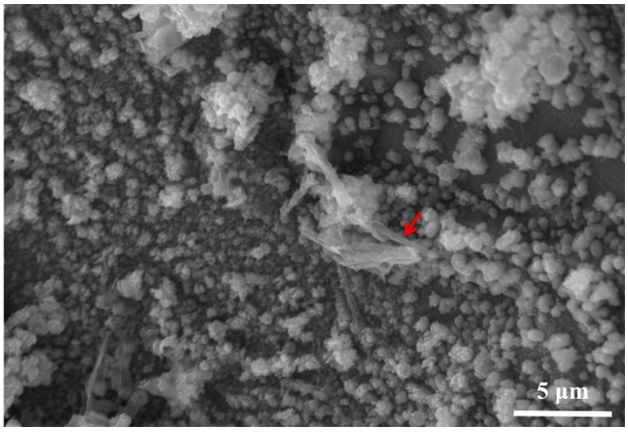


**Fig. S14** The SEM image of $CoMoO_4/MoO_3$@CuCoNi-S after 1500 cycles

**Table S1** Comparison of specific capacitance performance of similar materials at current density 1 A $g^{-1}$.

| Electrode materials | Specific capacitance (F $g^{-1}$) | References |
|---|---|---|
| C@$MoO_3$ | 179 | 1 |
| $MoO_3/MoS_2$ | 287.7 | 2 |
| $CoMoO_4$ | 384 | 3 |
| CuS@PPy | 427 | 4 |
| $MoO_3$/PANI | 632 | 5 |
| $CoMoO_4$@RGO | 856.2 | 6 |

| | | |
|---|---|---|
| CuS | 948 | 7 |
| $Co_9S_8$@$NiCo_2S_4$@NF | 1026 | 8 |
| $CoMoO_4$@$Ni(OH)_2$ | 1246 | 9 |
| $NiS_2$@Ni-Co-S | 1454 | 10 |
| $Co_9S_8$@NiO | 1627 | 11 |
| ZnS/$NiCo_2S_4$/$Co_9S_8$ | 1618.1 | 12 |
| $Co_9S_8$-MPA/NF | 1852 | 13 |
| ZnS/$Ni_3S_2$ | 2093 | 14 |
| $NiCo_2S_4$@$CoMoO_4$ | 2118.8 | 15 |
| CuS-rGO | 2317.8 | 16 |
| CoO@CoS/$Ni_3S_2$ | 2507 | 17 |
| $CoMoO_4$/$MoO_3$@CuCoNi-S | 2600 | This work |

**References**


1 Q. Wang, C. Zhou, X. H. Yan, J. J. Wang, D. F. Wang, X. X. Yuan and X. N. Cheng, *J Mater. Sci-Mater.El.,*2019,**30**,6643–6649.

2 S. V. Prabhakar Vattikuti, P. C. Nagajyothi, P. A. K. Reddy, M. K. Kumar, J. Shim and C. Byon, *Mater.Res.Let.,* 2018,**6**,432–441.

3 W. X. Li, X. W. Wang, Y. C. Hu, L. Y. Sun, C. Gao, C. C. Zhang, H. Liu and M. Duan, *Nanoscale Res.Lett.,* 2018,**13**,120.

4 H. Peng, G.F. Ma, K. J. Sun, J. J. Mu, H. Wang and Z. Q. Lei, *J. Mater. Chem. A,* 2014,**2**,3303–3307.

5 F. R. Jiang , W.Y. Li , R. J. Zou , Q. Liu , K.B. Xu, L. An and J. Q. Hu, *Nano Energy,* 2014,**7**,72–79.

6 J. L. Lv, M. Yang, K. Suzuki and H. Miura, *Micropor. Mesopor. Mat.,* 2017,**242**,264–270.

7 H.Heydari, S. E.Moosavifard and S. Elyasi, *Appl.Surf.Sci.,* 2017,**394**,425–430.

8 Y.Y.Yang, D.L. Qian, H. Zhu, Q.Zhou, Z.Y.Zhang, Z.M.Li and Z.G.Hu, *J Alloy.Compd.,* 2022,**898**,162850.

9 X. Wang, F. Rong, F. Huang, P. He, Y. Yang, J. Tang and R. Que, *J Alloy.Compd.,* 2019,**789**,684–692.

10 F. Zhang, J. Ma, Y. Qin, Y. Wang, S. Xu and R. Li, *Mater.Lett.,* 2020,**262**,127021.

11 J. M. Wang, Y. Huang, X. P. Han, S. Zhang, M. Y. Wang, J. Yan, C. Chen and M. Zong, *J Colloid Interf.Sci.,*2021,**603**,440–449.

12 Y. W. Sui, Y. M. Zhang, H. H. Hu, Q. Xu, F. Yang and Z. S. Li, *Adv. Mater. Interfaces,* 2018,**5**,1800018.

13 L.Li, Q.Li, J.Sun, Y.Y. Ling, K.Tao and L.Han, *Inorg.Chem.,* 2020,**59**,11174–11183.

14 X.X.Li, J.K.Sun, L.Y.Feng, L.J.Zhao, L.Ye, W.Q.Zhang and L.F.Duan, *J Alloy.Compd.,* 2018,**753**,508–516.

15 Y. Zhao, X. He, R. Chen, Q. Liu, J. Liu, D. Song, H. Zhang, H. Dong, R. Li, M. Zhang and J. Wang, *Appl.Surf.Sci.,*2018,**453**,73–82.

16 K.J.Huang, J.Z.Zhang, Y.Liu and Y.M.Liu,*Int.J Hydrogen Energ.,*2015,**40**,10158 – 10167.

17 Y. Zhang, D. Wang, S. Lü, Y. Chen, H. Fan, M. Wei, L. Yang, W.W. Yu and X. Meng, *Appl.Surf.Sci.,*2020,**532**,147438.